

LE-NeuS: Latency-Efficient Neuro-Symbolic Video Understanding via Adaptive Temporal Verification

Shawn Liang ¹	SHAWN.LIANG@CASE.EDU
Sahil Shah ²	SS96869@UTEXAS.EDU
Chengwei Zhou ¹	CHENGWEI.ZHOU@CASE.EDU
SP Sharan ²	SPSHARAN@UTEXAS.EDU
Harsh Goel ²	HARSHG99@UTEXAS.EDU
Arnab Sanyal ²	SANYAL@UTEXAS.EDU
Sandeep Chinchali ²	SANDEEPC@UTEXAS.EDU
Gourav Datta ¹	GOURAV.DATTA@CASE.EDU

¹Case Western Reserve University, ² The University of Texas at Austin

Abstract

Neuro-symbolic approaches to long-form video question answering (LVQA) have demonstrated significant accuracy improvements by grounding temporal reasoning in formal verification. However, existing methods incur prohibitive latency overheads, up to $90\times$ slower than Base VLM prompting, rendering them impractical for latency-sensitive edge deployments. We present **LE-NeuS**, a latency-efficient neuro-symbolic framework that preserves the accuracy benefits of temporal logic-guided video understanding while drastically reducing inference latency. Our key insight is that the dominant computational bottleneck arises from *sequential and dense proposition detection* across video frames during automaton construction. We address this through two principled optimizations: (1) **CLIP guided two-stage adaptive sampling** that exploits visual redundancy to skip semantically similar frames while preserving temporal boundaries, and (2) **batched proposition detection** that parallelizes VLM inference across temporal windows. Theoretically, we derive latency bounds as a function of video length, proposition complexity, and sampling density, establishing conditions under which latency efficiency is achievable. Empirically, on LongVideoBench and Video-MME benchmarks deployed on NVIDIA H100 GPUs, LE-NeuS reduces the latency gap from $90\times$ to approximately $10\times$ while maintaining $>\sim 10\%$ accuracy gains on temporally complex queries.

Keywords: neuro-symbolic, long-form video, model checking, CLIP, proposition

1. Introduction

The rapid growth of long-form video content has intensified the need for systems capable of answering complex, temporally grounded queries over extended horizons (Wu et al., 2024). Unlike static images or short clips, long-form video question answering (LVQA) requires the integration of three core capabilities: *semantic grounding* to identify entities and interactions, *temporal reasoning* to track events across long durations, and *compositional inference* to align multi-step reasoning with query structure. Although modern vision-language models (VLMs) have achieved strong performance in visual question answering (Bai et al., 2025; OpenGVLab, 2024; Achiam et al., 2023), they struggle with long-horizon compositional reasoning. Fixed context windows force aggressive frame down-sampling, often discarding subtle but crucial temporal transitions. Neuro-symbolic approaches such as NeuS-QA (Shah et al., 2025b) address this limitation by translating queries

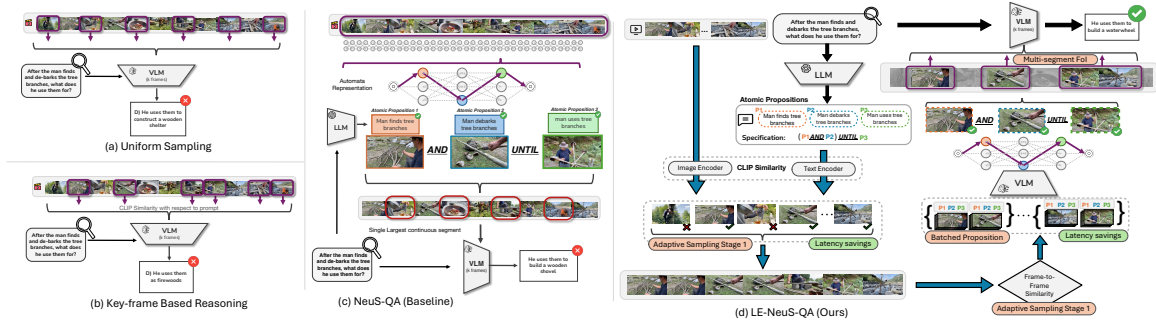


Figure 1: (a) **Vanilla VLM Prompting** uniformly samples a fixed number of frames across the entire video, irrespective of semantic relevance, which can omit critical temporal transitions and dilute reasoning with background content. (b) **Heuristic Retrieval** selects frames based on similarity to the query, improving relevance but lacking explicit temporal structure or formal reasoning guarantees. (c) **NeuS-QA (Baseline)** grounds atomic propositions over densely sampled frames, constructs a temporal logic specification, and performs formal model checking to retrieve a single continuous logic-satisfying segment; while principled and interpretable, this sequential grounding process incurs substantial latency overhead. (d) **LE-NeuS (Ours)** introduces *CLIP-guided adaptive sampling* and *batched proposition detection* to selectively ground propositions over semantically sparse, visually distinct keyframes. It *retrieves multiple high-density, logic-consistent segments* and performs verification with parallelized inference, achieving over an order-of-magnitude latency reduction while preserving formal reasoning guarantees and improving answer accuracy.

into temporal logic (TL) specifications and performing formal model checking to retrieve logically consistent segments. This structured reasoning paradigm yields substantial accuracy gains ($\sim 10\%$ on temporally complex categories in LongVideoBench) while offering interpretability and formal guarantees absent in heuristic retrieval methods (Choi et al., 2024). However, these benefits come at a significant computational cost: NeuS-QA incurs nearly $90\times$ higher latency than standard VLM prompting, limiting practical deployment.

Figure 1 summarizes this evolution. While *uniform sampling* and *heuristic retrieval* lack formal temporal guarantees, *NeuS-QA* introduces principled automaton-based verification at the expense of significant overhead. We propose **LE-NeuS**, a latency-efficient neuro-symbolic framework that preserves the strengths of TL-guided reasoning while substantially reducing inference cost. LE-NeuS achieves this through three complementary optimizations: (1) **Hierarchical Adaptive Sampling**, a two-stage CLIP-based filtering process that isolates semantically relevant regions and removes visually redundant frames; (2) **Parallel Proposition Detection**, which restructures automaton construction into batched VLM inference to fully utilize GPU throughput; and (3) **Multi-Segment Frames-of-Interest (FoI) Retrieval**, which concentrates the final VLM reasoning on high-density evidence segments rather than continuous spans. Evaluated on LongVideoBench, Video-MME, and MLVU using an NVIDIA H100 GPU, LE-NeuS achieves a $12.53\times$ global speedup, reducing average latency from $\sim 550s$ to $\sim 42s$, while improving accuracy by $\sim 4\%$ on complex temporal queries for videos up to one hour in length. Beyond empirical gains, we provide a formal latency analysis that characterizes the conditions under which neuro-symbolic video understanding can operate efficiently at scale.

2. Related Work

Long-Form Video Question Answering: Early VQA systems relied on fully supervised architectures encoding entire videos via convolutional and recurrent networks (Zhu et al., 2016; Ye et al., 2017; Jang et al., 2017; Antol et al., 2015). The emergence of large VLMs (Bai et al., 2025; OpenGVLab, 2024; Achiam et al., 2023; Li et al., 2024a,b) enabled zero-shot VQA with stronger generalization,

but these models typically consume fixed frame sets sampled from entire videos, limiting their ability to handle long-form content with complex temporal structure. Recent state-of-the-art approaches adopt retrieval-augmented strategies (Park et al., 2024; Wang et al., 2024; Ye et al., 2025; Wang et al., 2025; Song et al., 2024; Islam et al., 2025; Choudhury et al., 2023) that identify relevant video segments before querying VLMs. While effective at reducing irrelevant context, these methods rely on coarse heuristics or textual summarization that sacrifice visual fidelity and lack formal structure. **Neuro-Symbolic Video Understanding:** Symbolic representations have been explored across robotics (Puranic et al., 2021; Hasanbeig et al., 2019), autonomous vehicles (Zheng et al., 2025; Mehdipour et al., 2023; Shoukry et al., 2017), and structured neural networks (Manginas et al., 2024; Hashemi et al., 2023). In vision, symbolic methods support long-form understanding (Tapaswi et al., 2016; Huang et al., 2020; Xiong et al., 2019; Wu and Krähenbühl, 2021), though these typically rely on latent embeddings sacrificing interpretability. Previous works have pioneered the integration of temporal logic with neural perception for video understanding. Choi et al. (2024) introduced the foundational NSVS-TL framework that decouples perception from temporal reasoning through video automata. Yang et al. (2023) developed specification-driven video search combining foundation models with formal verification. Sharan et al. (2025) extended these ideas to text-to-video evaluation, demonstrating $5\times$ higher correlation with human judgments compared to existing metrics. Choi et al. (2025) further showed how neuro-symbolic feedback can improve video generation quality by 40%. Shah et al. (2025a) articulated the grand challenge of building neuro-symbolic video agents capable of temporal reasoning and action. Most recently, NeuS-QA (Shah et al., 2025b) achieved state-of-the-art results on LVQA benchmarks through temporal logic-guided segment retrieval, improving accuracy by over 10% on complex temporal queries. However, **none of these works address the latency implications** of neuro-symbolic pipelines, which is the focus of our work. *We offer the first systematic analysis of latency in neuro-symbolic video understanding and propose principled optimizations that enable a practical path toward real-time deployment.*

3. Preliminaries and Problem Formulation

3.1. Neuro-Symbolic Video Understanding

To introduce the idea of using logic for video understanding, we will use the running example—“*After the man goes into the forest, finds and debarks the tree branches, what does he use them for?*”

Temporal Logic Specifications: Let $\mathcal{P} = \{p_1, \dots, p_n\}$ denote a set of atomic propositions representing visual events in a natural language query q (for the running example, “man goes into the forest” “man finds tree branches” and “man debarks tree branches”, “man uses tree branches”). A temporal logic specification φ over \mathcal{P} is defined inductively (Baier and Katoen, 2008):

$$\varphi ::= p \mid \neg\varphi \mid \varphi_1 \wedge \varphi_2 \mid \varphi_1 \vee \varphi_2 \mid \diamond\varphi \mid \square\varphi \mid \varphi_1 \mathcal{U} \varphi_2 \mid \bigcirc\varphi \quad (1)$$

where $p \in \mathcal{P}$, \diamond (eventually), \square (always), \mathcal{U} (until), and \bigcirc (next) are temporal operators. An illustration of this process is shown in Figure 2. The specification encodes the temporal structure of the query; for instance our running example translates to $\varphi = (p_{\text{going into forest}} \wedge (p_{\text{finds branches}} \wedge p_{\text{debark branches}})) \mathcal{U} (p_{\text{use branches}})$.

Video Automaton: Following the framework of NeuS-QA (Choi et al., 2024; Shah et al., 2025b), a video V of length T is modeled as a discrete-time Markov chain automaton: $\mathcal{A}_V = (Q, q_0, \delta, \lambda)$, constructed incrementally by processing the video stream in discrete frame windows of size κ . Here, $Q = \{q_0, q_1, \dots, q_N\}$ is the state set, where each state q_t corresponds to a sampled frame window \mathcal{F}_t

of κ consecutive frames. This window size κ serves as the temporal granularity for the state-based model, enabling the VLM to capture the evolution of identified events (e.g., “finds tree branches”) within the window (Shah et al., 2025b). The transition function $\delta(q_t, q_{t+1}) = 1$ enforces sequential progression, while the labeling function $\lambda : Q \rightarrow [0, 1]^{|\mathcal{P}|}$ assigns atomic propositions to each state based on VLM detection confidence.

Probabilistic Model Checking: Given \mathcal{A}_V and specification φ , probabilistic model checking (Baier and Katoen, 2008; Clarke et al., 1999) computes the satisfaction probability: $P_{\text{sat}} = \mathbb{P}[\mathcal{A}_V \models \varphi]$, using tools such as Storm (Hensel et al., 2020). A satisfying path $\pi = q_{t_1} \rightarrow q_{t_2} \rightarrow \dots \rightarrow q_{t_k}$ identifies the video segment containing query-relevant events, which is then provided to a VLM for final answer generation.

3.2. Latency Decomposition and Bottleneck Analysis

To identify the primary drivers of processing delay, we first decompose end-to-end latency into main functional stages.

Definition 1 (NeuS Pipeline Latency) *The end-to-end latency $\mathcal{L}_{\text{NeuS}}$ of a neuro-symbolic video understanding pipeline consists of four additive components as $\mathcal{L}_{\text{NeuS}} = \mathcal{L}_{\text{LQ2TL}} + \mathcal{L}_{\text{auto}} + \mathcal{L}_{\text{MC}} + \mathcal{L}_{\text{VQA}}$, where $\mathcal{L}_{\text{LQ2TL}}$, $\mathcal{L}_{\text{auto}}$, \mathcal{L}_{MC} , and \mathcal{L}_{VQA} represent the latencies for query-to-TL translation, automaton construction, symbolic model checking, and final VQA answering, respectively.*

Although several stages remain relatively constant regardless of video duration, collectively denoted as the fixed overhead $\mathcal{L}_{\text{fixed}} = \mathcal{L}_{\text{LQ2TL}} + \mathcal{L}_{\text{MC}} + \mathcal{L}_{\text{VQA}}$, $\mathcal{L}_{\text{auto}}$ scales directly with video length T since it requires a VLM to ground frame-level propositions into states for automaton construction.

Definition 2 (Sequential Automaton Construction Latency) *Given the automaton \mathcal{A}_V constructed over frame windows of size κ , the latency of evaluating all atomic propositions \mathcal{P} via sequential VLM polling is derived as: $\mathcal{L}_{\text{auto}}^{\text{seq}} = \lceil \frac{T}{\kappa} \rceil \cdot |\mathcal{P}| \cdot \mathcal{L}_{\text{prop}}$, where $\lceil T/\kappa \rceil$ represents the total number of state units (windows) and $\mathcal{L}_{\text{prop}}$ denotes the inference latency for a single proposition-window pair. This scaling with respect to both video length and proposition count constitutes the primary computational bottleneck in the baseline framework (Shah et al., 2025b).*

As T increases, $\mathcal{L}_{\text{auto}}^{\text{seq}}$ shifts from a sub-dominant task to the primary computational bottleneck. Specifically, the automaton construction latency dominates the total processing time (i.e., $\mathcal{L}_{\text{auto}}^{\text{seq}} > \mathcal{L}_{\text{fixed}}$) whenever the video duration exceeds a critical threshold T_{crit} , derived by substituting the definition of $\mathcal{L}_{\text{auto}}^{\text{seq}}$ into the inequality and solving for T . T_{crit} is computed as $T_{\text{crit}} = \frac{\kappa \cdot \mathcal{L}_{\text{fixed}}}{|\mathcal{P}| \cdot \mathcal{L}_{\text{prop}}}$.

Problem Statement: Given a video V and query q , we aim to design a segment retrieval strategy that minimizes computational overhead while preserving reasoning accuracy. The method must: (i) **Satisfy Logical Constraints** by identifying segments $S \subseteq V$ that satisfy the temporal logic specification φ ; (ii) **Reduce Latency** by significantly lowering automaton construction time $\mathcal{L}_{\text{auto}}$; and (iii) **Maximize Hardware Utilization** through parallel execution to efficiently leverage modern GPU architectures.

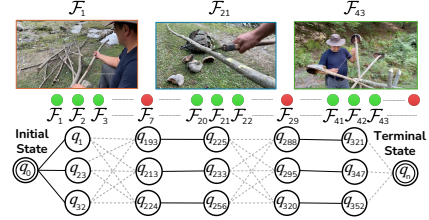


Figure 2: Video automaton for the running example: “After the man goes into the forest, finds and debarks the tree branches, what does he use them for?” **Top:** representative frames for key events (entering the forest, finding and debarking branches, and using them). **Bottom:** finite-state automaton derived from the temporal logic specification φ . Green states indicate frames where relevant atomic propositions are detected and temporal constraints remain satisfied; red states denote irrelevant frames or transitions that violate φ . Incremental verification ensures that only runs $\rho \models \varphi$ are retained, and reaching the accepting state yields a witness segment satisfying the query.

4. Proposed Method

We introduce LE-NeuS, a latency-efficient neuro-symbolic framework that targets the primary bottleneck in prior pipelines: sequential automaton construction and dense proposition grounding. LE-NeuS restructures this process to exploit semantic sparsity, visual redundancy, and task-level parallelism while preserving temporal logic guarantees. As illustrated in Figure 1(d), adaptive sampling is applied prior to automaton construction to reduce the number of grounded states without altering formal verification. Given a video V and query q , LE-NeuS translates q into a temporal logic specification φ with atomic propositions \mathcal{P} . A lightweight encoder extracts a sparse keyframe set \mathcal{K} , over which propositions are evaluated in parallel using batched VLM inference. Probabilistic model checking then identifies segments \mathcal{S} satisfying φ , and the final answer is generated from these verified segments. Unlike NeuS-QA (Shah et al., 2025b), which performs dense sequential grounding, LE-NeuS applies selective and parallel inference to achieve substantial latency reductions. The full pipeline is summarized in Algorithm 1.

Batched Proposition Detection: The baseline `NeuS-QA` implementation evaluates propositions sequentially for each window, treating each (Window, Proposition) pair as a separate inference call. This approach severely underutilizes modern GPU resources, as the overhead of kernel launching and weight loading is incurred repeatedly for small workloads. LE-NeuS-QA addresses this by employing standard batched inference, where multiple proposition-window pairs are stacked along the batch dimension and processed in a single forward pass.

Definition 3 (Batched Proposition-Window Pair Evaluation) *Let \mathcal{F}_t denote a frame window and $\mathcal{P} = \{p_1, \dots, p_{|\mathcal{P}|}\}$ be the set of atomic propositions. We construct a batch \mathcal{B}_t of size B consisting of duplicated visual contexts paired with distinct propositions: $\mathcal{B}_t = (\mathcal{F}_t, p_i) \mid i \in 1, \dots, B$. Crucially, since the visual input \mathcal{F}_t is constant across the batch, its visual features are computed only once and effectively broadcast across the concurrent proposition queries, eliminating redundant vision encoder operations. The batched detection function $\mathcal{M}_{batch} : (\text{Frames} \times \text{Text})^B \rightarrow [0, 1]^B$ computes confidence scores for the entire batch simultaneously: $\mathbf{Z}_{batch} = \mathcal{M}_{batch}(\mathcal{B}_t)$ where the i -th output corresponds to the confidence of proposition p_i given window \mathcal{F}_t .*

In this standard batching formulation, the primary constraint is GPU VRAM. The memory must accommodate the static model weights alongside the dynamic activation maps and KV-caches for B concurrent sequences. This strategy yields a substantial throughput increase: whereas sequential processing requires $|\mathcal{P}|$ independent forward passes (and visual encodings) per window, batched processing reduces this to $\lceil |\mathcal{P}|/B \rceil$ passes. On compute-bound hardware, this effectively amortizes the fixed costs of inference across the batch, leading to a speedup factor that approaches B for large proposition sets.

CLIP-Guided Two-Stage Adaptive Sampling: While batching improves throughput, processing every frame sampled uniformly regardless of the video length remains a significant bottleneck. We address this by leveraging the inherent semantic and visual sparsity of long-form video, where valid propositions \mathcal{P} typically appear in short, sparse intervals surrounded by redundant background content. We replace uniform sampling with a hierarchical two-phase pipeline using CLIP embeddings (Radford et al., 2021) as a lightweight proxy for similarity. All embeddings are ℓ_2 -normalized to the unit hyper-sphere, enabling efficient dot-product similarity computations, maximizing inference throughput.

Stage 1: Semantic Relevance Filtering: We utilize the CLIP ViT-B/32 image (CLIP_V) and text (CLIP_T) encoders to project frames and propositions into a shared 512-dimensional latent space.

Definition 4 (Semantic Relevancy Score) Let $\mathbf{z}_{f_t} = \frac{CLIP_V(f_t)}{\|CLIP_V(f_t)\|_2}$ and $\mathbf{z}_{p_i} = \frac{CLIP_T(p_i)}{\|CLIP_T(p_i)\|_2}$ be the ℓ_2 -normalized visual and textual embeddings. The pairwise similarity score is defined as the dot product: $\text{sim}(f_t, p_i) = \mathbf{z}_{f_t}^\top \mathbf{z}_{p_i}$.

To identify segments aligned with the target set \mathcal{P} , we compute a coarse relevancy score s_t for each frame by taking the maximum similarity across all propositions: $s_t = \max_{p_j \in \mathcal{P}} \text{sim}(f_t, p_j)$. Frames exceeding a threshold τ_s are retained and temporally expanded by a radius w (total window $2w$) to preserve context. Finally, overlapping segments are merged to form the candidate set \mathcal{F}_{cand} , effectively pruning irrelevant background content.

Stage 2: Visual Redundancy Elimination: Within \mathcal{F}_{cand} , we perform a second pass to eliminate near-duplicate frames, ensuring heavy VLM inference is reserved only for distinct *informative* frames.

Definition 5 (Visual Redundancy Score) For consecutive frames $f_t, f_{t+1} \in \mathcal{F}_{cand}$, the redundancy score r is defined as the dot product of their normalized visual embeddings: $r(f_t, f_{t+1}) = \mathbf{z}_{f_t}^\top \mathbf{z}_{f_{t+1}}$.

Definition 6 (Sequential Adaptive Keyframe Selection) Let $\mathcal{F}_{cand} = \{f_1, f_2, \dots, f_M\}$ be the temporally ordered candidate frames. We construct the keyframe set \mathcal{K} iteratively. Initialize $\mathcal{K} = \{f_1\}$ and set the current comparison base $f_{base} = f_1$. For each subsequent frame $f_t \in \mathcal{F}_{cand}$, we compute the redundancy score $r(f_{base}, f_t)$. If $r(f_{base}, f_t) < \tau_r$ (indicating significant visual change), then f_t is added to \mathcal{K} and the comparison base is updated: $f_{base} \leftarrow f_t$. Otherwise, f_t is discarded.

The threshold τ_r controls the tradeoff between latency and temporal precision; we find $\tau_r = 0.9$ provides an optimal balance across diverse video types. In the final *dense detection phase*, we perform proposition detection only on these keyframes and their local neighborhoods. Formally, $\mathcal{F}_{detect} = \bigcup_{k \in \mathcal{K}} f_t : |t - k| \leq \delta$, where $\delta = 2$. For frames $f_t \notin \mathcal{F}_{detect}$, we propagate proposition labels from the preceding keyframe. This label propagation is justified by the sequential construction of \mathcal{K} ; since f_t was discarded due to high similarity with its preceding base keyframe f_{base} , we assume $\lambda(p_i, f_t) \approx \lambda(p_i, f_{base})$, allowing the model checker to inherit labels without explicit VLM inference.

Automaton Construction and Verification: With proposition detections Z computed over keyframes and propagated to remaining frames, we construct the video automaton \mathcal{A}_V following the standard procedure (Shah et al., 2025b; Choi et al., 2024). Each frame window F_t corresponds to a state q_t in a discrete-time Markov chain \mathcal{A}_V , where labeling is grounded in calibrated probabilistic detections $Z_{t,i} \in [0, 1]$. We employ the Storm (Hensel et al., 2020) model checker to compute satisfaction probabilities P_t , which are subsequently refined via a sigmoid smoothing function $F_b(\cdot)$ to suppress low-confidence noise. This identifies a minimal satisfying interval, which we extend by temporal offsets (α, β) to ensure the final VLM has sufficient lead-up and aftermath context for the question.

Multi-Segment FoI Retrieval Strategy: We enhance the LQ2TL stage to support flexible temporal logic mappings, enabling LE-NeuS to generalize across compositional query types, particularly those involving identifying temporal ordering of a sequence of events. Unlike prior NeuS-QA pipelines that extract only the single largest continuous satisfying window, LE-NeuS returns a list of disjoint segments corresponding to the specific intervals where the specification and propositions hold. We formalize the advantage of this strategy through sampling probability. Let N be the fixed frame budget of the VLM, $|E|$ the count of true evidence frames, and $|\mathcal{V}_{total}|$ the total frame count in the retrieved context. The probability of sampling at least one evidence frame is computed as $P(\text{Hit}) \approx 1 - \left(1 - \frac{|E|}{|\mathcal{V}_{total}|}\right)^N$. Under this formulation, the retrieval mechanism reduces the denominator $|\mathcal{V}_{total}|$ by excluding the temporal gaps between non-adjacent events. Consequently, the fixed sampling budget N is allocated exclusively to the disjoint intervals identified by the automaton,

Algorithm 1 LE-NeuS: Latency-Efficient Neuro-Symbolic Video Understanding

Input: Video $V = \{f_1, \dots, f_T\}$, query q , batch size B , thresholds $\{\tau_s, \tau_r\}$, window w

Output: Answer \hat{c}

```

1:  $\mathcal{P}, \varphi \leftarrow \text{LQ2TL}(q)$                                 {Translate query to Temporal Logic}
2:  $\{e_t\}_{t=1}^T \leftarrow \text{CLIP}_V(V)$                         {Batched image encoding}
3:  $\mathcal{F}_{cand} \leftarrow \{f_t : \max_{p \in \mathcal{P}} \cos(e_t, \text{CLIP}_T(p)) > \tau_s\}$     {Phase 1: Semantic Filtering}
4:  $\mathcal{K} \leftarrow \{f_1\}, f_{base} \leftarrow f_1$ 
5: for each  $f_t \in \mathcal{F}_{cand}$  do
6:   if  $\cos(e_{base}, e_t) < \tau_r$  then
7:      $\mathcal{K} \leftarrow \mathcal{K} \cup \{f_t\}, f_{base} \leftarrow f_t$     {Phase 2: Visual Redundancy Elimination}
8:   end if
9: end for
10:  $\mathcal{F}_{detect} \leftarrow \bigcup_{k \in \mathcal{K}} \{f_t : |t - k| \leq \delta\}$     {Expand to local neighborhoods}
11: Initialize detection matrix  $Z \in [0, 1]^{T \times |\mathcal{P}|}$ 
12: for each window  $F_t$  centered at  $f_t \in \mathcal{F}_{detect}$  with size  $\kappa$  do
13:    $Z[t, :] \leftarrow \text{VLM}_{batch}(f_t, \mathcal{P})$ 
14: end for
15:  $\mathcal{A}_V \leftarrow \text{BuildAutomaton}(Z)$                                 {Symbolic grounding}
16:  $P_{sat}, \pi^* \leftarrow \text{Storm}(\mathcal{A}_V, \varphi)$                     {Formal model checking}
17:  $S \leftarrow \text{ExtractSegment}(\pi^*, \alpha, \beta)$                 {Identify evidence clip}
18:  $\hat{c} \leftarrow \text{VLM}_{answer}(q, S)$                             {Final multimodal reasoning}
19: return  $\hat{c}$ 

```

rather than being distributed across the full continuous span required to encompass the start and end of the sequence.

5. Theoretical Analysis

We formally characterize the computational complexity of the pipeline and derive an upper bound for the end-to-end inference latency.

Theorem 7 (LE-NeuS Latency Bound) *The end-to-end latency of LE-NeuS is bounded by*

$$\mathcal{L}_{LE-NeuS} \leq \mathcal{L}_{LQ2TL} + T \cdot \mathcal{L}_{CLIP} + \lceil \frac{\alpha \rho T}{k} \rceil \cdot \mathcal{L}_{VLM} + \mathcal{L}_{MC} + \mathcal{L}_{VQA} \quad (2)$$

where α is the ratio of frames retained after semantic filtering, defined as $\alpha = \frac{|\mathcal{F}_{cand}|}{T}$, ρ is the keyframe retention rate, defined as the ratio of unique keyframes retained from the candidate set: $\rho = \frac{|\mathcal{K}|}{|\mathcal{F}_{cand}|}$, and $\mathcal{L}_{CLIP}, \mathcal{L}_{VLM}$ are per-frame CLIP and VLM latencies respectively.

The bound follows from summing the latency contributions of each pipeline stage: (1) LQ2TL translation; (2) CLIP encoding of all frames, contributing $T \cdot \mathcal{L}_{CLIP}$; (3) Batched proposition detection is performed on the identified keyframes, contributing $\lceil \alpha \rho T \rceil \cdot \mathcal{L}_{VLM}$, where $\alpha \rho T$ represents the total count of retained keyframes $|\mathcal{K}|$; (4) Model checking; (5) Final VQA.

Theorem 8 (Condition for Latency Efficiency) *LE-NeuS achieves latency efficiency ($\mathcal{L} \leq \mathcal{L}_{max}$) when $\alpha \rho \leq \frac{\mathcal{L}_{max} - \mathcal{L}_{fixed} - T \cdot \mathcal{L}_{CLIP}}{N_{win} \cdot \mathcal{L}_{VLM}}$, where $N_{win} = \lceil T/\kappa \rceil$ is the total number of frame windows in the video, and $\mathcal{L}_{fixed} = \mathcal{L}_{LQ2TL} + \mathcal{L}_{MC} + \mathcal{L}_{VQA}$ represents the fixed overhead.*

This condition highlights the core trade-off: latency efficiency depends on the joint density ($\alpha\rho$), now defined as the fraction of total video windows that are actually processed.

Proposition 9 (Speedup over Baseline) *The theoretical speedup of LE-NeuS over the baseline NeuS-QA implementation computed as $\frac{\mathcal{L}_{\text{auto}}^{\text{seq}}}{\mathcal{L}_{\text{auto}}^{\text{LE-NeuS}}} \approx \frac{|\mathcal{P}|}{\alpha\rho} \cdot \frac{1}{1 + \frac{T \cdot \mathcal{L}_{\text{CLIP}}}{N_{\text{win}} \cdot \mathcal{L}_{\text{VLM}}}}$.*

The proof is provided in Appendix A. For typical values where $|\mathcal{P}| = 5$ and the window retention rate is 5% ($\alpha\rho = 0.05$), the theoretical speedup approaches $100\times$, driven by the multiplicative benefits of proposition batching and adaptive sampling.

6. Experiments

We evaluate the effectiveness and efficiency of LE-NeuS for LVQA, demonstrating substantial reductions in latency while preserving rigorous logical reasoning for complex temporal queries.

Implementation Details: For automaton construction, we use InternVL2-8B (OpenGVLab, 2024) to ground atomic propositions \mathcal{P} across frames. Temporal logic translation (LQ2TL) is performed using GPT-4o (Achiam et al., 2023) with a flexible prompt template for compositional queries. Adaptive sampling employs CLIP ViT-B/32 embeddings with thresholds $\tau_s = 0.21$ and $\tau_r = 0.9$. Following Shah et al. (2025b), we use the stormpy (Junges and Volk, 2021) probabilistic model checker for TL verification. All latency results are measured end-to-end on a single NVIDIA H100 GPU, including LQ2TL translation time ($\mathcal{L}_{\text{LQ2TL}}$).

Evaluation Backbones & Baselines. We evaluate LE-NeuS with four state-of-the-art VLM backbones for final VQA: InternVL2.5-8B, Qwen2.5-VL-7B, VideoLLaMA3-7B, and LLaVA-Video-7B. Comparisons include: (i) Base VLMs with uniform frame sampling, (ii) the original NeuS-QA (Shah et al., 2025b) on the same backbones, and (iii) structured reasoning methods, including T* (Ye et al., 2025), VideoTree (Wang et al., 2025), VideoAgent (Wang et al., 2024), and LVNet (Park et al., 2024), evaluated on LongVideoBench. All experiments use the `lmms-eval` framework (Zhang et al., 2024), with subtitles burned into frames for consistent multimodal grounding.

Benchmarks: We primarily evaluate LE-NeuS on LongVideoBench (Wu et al., 2024), comparing against Base VLMs, NeuS-QA, and structured reasoning baselines. Following Shah et al. (2025b), we focus on the reasoning-intensive subsets (T3E, E3E, T3O, O3O), featuring videos up to 60 minutes that require temporal ordering, causal inference, and compositional reasoning. To further assess architectural strengths, we conduct targeted diagnostics on Video-MME (Fu et al., 2024) (Temporal Reasoning category) and MLVU (Zhou et al., 2025), using Needle QA to test sparse retrieval in long contexts and Ego Reasoning to evaluate action-sequence understanding. Across all datasets, subtitles are burned into frames following the NeuS-QA protocol to ensure consistent multimodal grounding.

Accuracy Results: Table 1 and Figure 3 present the performance of LE-NeuS across our primary and diagnostic benchmarks. On LongVideoBench, LE-NeuS establishes a new state-of-the-art across all evaluated backbones. Most notably, using the InternVL2.5-8B model, our framework achieves a peak overall accuracy of 67.10%, surpassing the NeuS-QA baseline (61.89%) by a significant margin of 5.21%. Critically, LE-NeuS demonstrates an advantage over all structured reasoning frameworks, outperforming the best framework, VideoTree (50.47%), by over 16%. This architectural advantage extends to the diagnostic benchmarks shown in Figure 3. On Video-MME, LE-NeuS demonstrates superior long-horizon modeling, achieving 67.24% on Temporal Reasoning

Framework	Model	LongVideoBench				
		T3E	E3E	T3O	O3O	Overall
Base VLM	InternVL2.5-8B	58.90	71.28	50.00	54.55	59.61
	VideoLLaMA3-7B	60.27	61.70	58.11	50.0	57.98
	LLaVA-Video-7B-Qwen2	46.58	55.32	55.41	39.39	49.84
	Qwen2.5-VL-7B-Instruct	46.58	63.83	56.78	53.03	55.70
Structured Reasoning Frameworks	VideoTree (Wang et al. (2025))	56.38	50.00	50.00	43.84	50.47
	LVNet (Park et al. (2024))	41.94	54.17	35.48	46.15	45.59
	VideoAgent (Wang et al. (2024))	45.45	52.63	27.27	27.27	40.38
	T* (Ye et al. (2025))	28.95	35.56	48.33	22.22	35.75
NeuS-QA	NeuS-QA + InternVL2.5-8B	58.91	69.15	58.11	59.09	61.89
	NeuS-QA + VideoLLaMA3-7B	56.16	68.09	59.46	62.12	61.89
	NeuS-QA + LLaVA-Video-7B-Qwen2	54.80	58.51	55.41	45.48	54.07
	NeuS-QA + Qwen2.5-VL-7B-Instruct	57.53	70.21	60.81	54.55	61.56
LE-NeuS (Ours)	InternVL2.5-8B	64.39	76.60	60.81	63.64	67.10
	LE-NeuS + VideoLLaMA3-7B	64.38	74.47	70.27	54.55	66.76
	LE-NeuS + LLaVA-Video-7B-Qwen2	57.53	61.70	50.00	45.46	54.40
	LE-NeuS + Qwen2.5-VL-7B-Instruct	68.09	56.16	64.87	65.15	63.84

Table 1: Top-1 Accuracy (%) on 4 complex-reasoning subsets of LongVideoBench. We evaluate **LE-NeuS** against the NeuS-QA baseline and Base VLM inference across four state-of-the-art backbones. **LE-NeuS** consistently achieves superior performance, notably surpassing NeuS-QA by 5.21% on LongVideoBench.

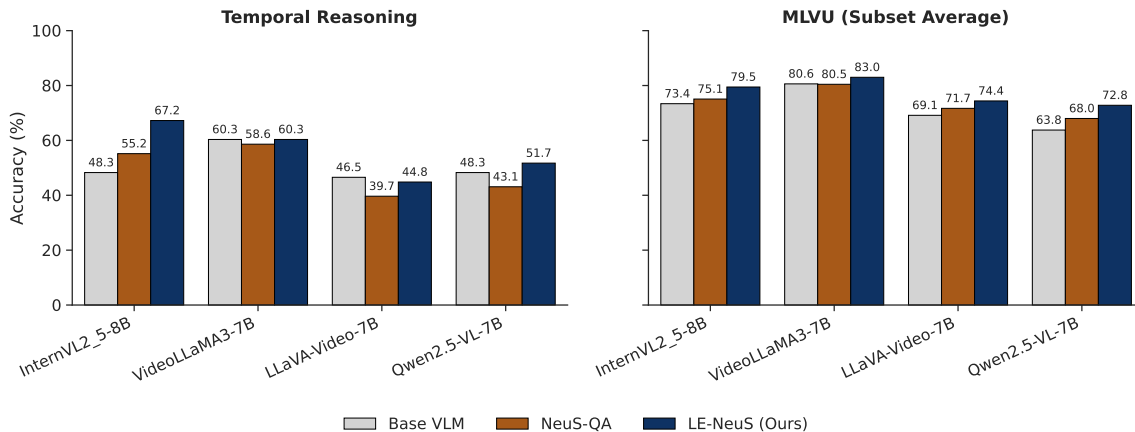


Figure 3: Top-1 Accuracy (%) on Video-MME, and MLVU. We evaluate **LE-NeuS** against the NeuS-QA baseline and Base VLM inference for subsets of Video-MME and MLVU. **LE-NeuS** consistently achieves superior performance, surpassing Base-VLM and NeuS-QA across all question subsets.

(InternVL2.5-8B)—a 12.07% improvement over NeuS-QA. Furthermore, on MLVU Ego-Reasoning and Needle-QA subsets, our framework consistently leads across all backbones. This consistent performance gain validates that our Multi-Segment FoI Retrieval strategy maximizes the evidence frames ratio, effectively concentrating the VLM’s attention on high-density evidence frames that are otherwise lost in continuous-window baselines.

Efficiency and Latency Analysis: Table 2 details the computational efficiency of LE-NeuS compared to the NeuS-QA baseline and standard VLM inference across varying video durations. While NeuS-QA suffers from linear latency scaling, reaching an impractical 957.80s (~ 16 minutes) for 60-minute videos due to processing an average of 1,427 frames, LE-NeuS maintains a robust sub-linear profile. For the same 3,600s duration, our framework completes inference in just 70.01s, utilizing only 281 highly relevant frames. This translates to a $13.66\times$ speedup for long-form content. On a

Video Length (T)	Avg. Total Frames Used			Avg. FOI % of Video			Avg. Completion Time (s)			
	Standard VLM	NeuS-QA	LE-NeuS	Standard VLM	NeuS-QA	LE-NeuS	Standard VLM	NeuS-QA	LE-NeuS	Speedup
15 (Short)	32	44	59	–	87.80%	85.77%	4.15	10.25	5.47	1.87×
60 (Medium)	32	71	110	–	77.90%	65.43%	4.15	27.24	9.03	3.01×
600 (Medium-Long)	32	422	158	–	37.90%	31.86%	4.15	332.17	30.59	10.86×
3600 (Long)	32	1427	281	–	24.51%	20.53%	4.15	957.80	70.01	13.66×
Global Average	32	824	197	–	42.81%	37.35%	4.15	553.68	44.20	12.53×

Table 2: Latency Comparison between standard VLM vs. NeuS-QA vs. LE-NeuS assuming standard VLM uses 32 frames uniform sampling.

Method	Batching	Adaptive	Multi-Seg	Avg. Windows	Avg. VLM Calls	Accuracy	Latency (s)
Baseline (NeuS-QA)	-	-	-	268	1206	61.98	553.68
+ Batched Proposition Detection	✓	-	-	268	268	61.19	171.05
+ Adaptive Sampling	✓	✓	-	56	56	60.18	45.28
LE-NeuS (Ours)	✓	✓	✓	56	56	67.10	44.20

Table 3: **Ablation Study of LE-NeuS Components.** We report the global average VLM window count and latency alongside QA accuracy. *Batching* denotes Batched proposition detection. *Adaptive* refers to our two-stage CLIP adaptive sampling. *Multi-Seg* indicates the Multi-Segment FoI Retrieval Strategy.

global average, LE-NeuS achieves a 12.53× speedup over the baseline, reducing the average total frame count from 824 to 197 while simultaneously narrowing the Frames of Interest (FOI) percentage from 42.81% to 37.35%. This reduction confirms that our adaptive sampling strategy effectively prunes redundant temporal segments, decoupling inference cost from video length and enabling practical neuro-symbolic reasoning on extensive video streams.

Ablation Studies: Table 3 analyzes each component of LE-NeuS. The baseline (NeuS-QA) exhibits high latency (553.68s) due to sequential VLM calls. Adding **Batched Proposition Detection** reduces latency to 171.05s (3.2× speedup) with minimal accuracy change (61.19%). Incorporating **Adaptive Sampling** further lowers latency to 45.28s (3.8× additional speedup) by reducing processed windows from 268 to 56, with a slight accuracy drop (61.19% → 60.18%) due to aggressive pruning. Finally, **Multi-Segment FoI Retrieval** improves accuracy to **67.10%** (+6.92%) while maintaining low latency. Overall, LE-NeuS achieves a 12.53× latency reduction and a +5.12% absolute accuracy gain over the baseline.

7. Conclusions and Discussions

We introduced LE-NeuS, a latency-efficient neuro-symbolic framework for long-form video question answering. By identifying automaton construction as the primary bottleneck and restructuring it with batched proposition detection and CLIP-guided adaptive sampling, LE-NeuS reduces latency overhead from $\sim 90\times$ to $\sim 10\times$ while preserving the accuracy and interpretability of temporal logic reasoning. Although performance still depends on VLM-based grounding and specification complexity, a clear path toward near-real-time performance exists. Lightweight, task-specific proposition detectors could shrink the dominant inference cost; neural approximations of probabilistic model checking could amortize verification; and speculative, query-conditioned automaton construction could enable early termination without exhaustive grounding.

While demonstrated on LVQA, a task that already requires responsive reasoning over long-form video, the principles of LE-NeuS extend to other latency-critical video systems where structured temporal reasoning must operate under strict budgets. Similar constraints arise in embodied and agentic systems verifying multi-step execution, autonomous driving with temporally consistent event validation, wearable assistive vision for safety-critical cues, and edge monitoring scenarios. In these settings, selectively grounding propositions and verifying temporal constraints, rather than densely processing entire streams, enables logic-aware decision-making without sacrificing responsiveness.

References

- Josh Achiam, Steven Adler, Sandhini Agarwal, Lama Ahmad, Ilge Akkaya, Florencia Leoni Aleman, Diogo Almeida, Janko Altenschmidt, Sam Altman, Shyamal Anadkat, et al. GPT-4 technical report. *arXiv preprint arXiv:2303.08774*, 2023.
- Stanislaw Antol, Aishwarya Agrawal, Jiasen Lu, Margaret Mitchell, Dhruv Batra, C Lawrence Zitnick, and Devi Parikh. VQA: Visual question answering. In *Proceedings of the IEEE International Conference on Computer Vision (ICCV)*, pages 2425–2433, 2015.
- Shuai Bai, Keqing Chen, Xuecheng Liu, Jialin Wang, Wenbin Ge, Shuai Song, Kai Dang, Peng Wang, Shijie Wang, Jun Tang, et al. Qwen2.5-VL technical report. *arXiv preprint arXiv:2502.13923*, 2025.
- Christel Baier and Joost-Pieter Katoen. *Principles of Model Checking*. MIT Press, 2008.
- Minkyu Choi, Harsh Goel, Mohammad Omama, Yunhao Yang, Sahil Shah, and Sandeep Chinchali. Towards neuro-symbolic video understanding. In *European Conference on Computer Vision (ECCV)*, pages 220–236. Springer, 2024.
- Minkyu Choi, S P Sharan, Harsh Goel, Sahil Shah, and Sandeep Chinchali. We’ll fix it in post: Improving text-to-video generation with neuro-symbolic feedback. *arXiv preprint arXiv:2504.17180*, 2025.
- Rohan Choudhury, Koichiro Niinuma, Kris M Kitani, and Laszlo A Jeni. Zero-shot video question answering with procedural programs. *arXiv preprint arXiv:2312.00937*, 2023.
- Edmund M Clarke, Orna Grumberg, and Doron A Peled. *Model Checking*. MIT Press, 1999.
- Chaoyou Fu, Yuhan Dai, Yongdong Luo, Lei Li, Shuhuai Ren, Renrui Zhang, Zihan Wang, Chenyu Zhou, Yunhang Shen, Mengdan Zhang, et al. Video-mme: The first-ever comprehensive evaluation benchmark of multi-modal llms in video analysis. *arXiv preprint arXiv:2405.21075*, 2024.
- Mohammadhosein Hasanbeig, Yiannis Kantaros, Alessandro Abate, Daniel Kroening, George J Pappas, and Insup Lee. Reinforcement learning for temporal logic control synthesis with probabilistic satisfaction guarantees. In *IEEE 58th Conference on Decision and Control (CDC)*, pages 5338–5343. IEEE, 2019.
- Navid Hashemi, Bardh Hoxha, Tony Yamaguchi, Danil Prokhorov, Georgios Fainekos, and Jyotirmoy Deshmukh. A neurosymbolic approach to the verification of temporal logic properties of learning-enabled control systems. In *Proceedings of the ACM/IEEE 14th International Conference on Cyber-Physical Systems (ICCPS)*, pages 98–109, 2023.
- Christian Hensel, Sebastian Junges, Joost-Pieter Katoen, Tim Quatmann, and Matthias Volk. The probabilistic model checker Storm. *arXiv preprint arXiv:2002.07080*, 2020.
- Qingqiu Huang, Yu Xiong, Anyi Rao, Jiaze Wang, and Dahua Lin. MovieNet: A holistic dataset for movie understanding. In *European Conference on Computer Vision (ECCV)*, pages 709–727. Springer, 2020.

- Md Mohaiminul Islam, Tushar Nagarajan, Huiyu Wang, Gedas Bertasius, and Lorenzo Torresani. Bimba: Selective-scan compression for long-range video question answering. In *Proceedings of the IEEE/CVF Conference on Computer Vision and Pattern Recognition (CVPR)*, pages 29096–29107, 2025.
- Yunseok Jang, Yale Song, Youngjae Yu, Youngjin Kim, and Gunhee Kim. TGIF-QA: Toward spatio-temporal reasoning in visual question answering. In *Proceedings of the IEEE Conference on Computer Vision and Pattern Recognition (CVPR)*, pages 2758–2766, 2017.
- Sebastian Junges and Matthias Volk. Stormpy – Python bindings for Storm. <https://github.com/moves-rwth/stormpy>, 2021.
- Bo Li, Yuanhan Zhang, Dong Guo, Renrui Zhang, Feng Li, Hao Zhang, Kaichen Zhang, Peiyuan Zhang, Yanwei Li, Ziwei Liu, et al. LLaVA-OneVision: Easy visual task transfer. *arXiv preprint arXiv:2408.03326*, 2024a.
- Dongxu Li, Yudong Liu, Haoning Wu, Yue Wang, Zhiqi Shen, Bowen Qu, Xinyao Niu, Fan Zhou, Chao Huang, Yanwei Li, et al. Aria: An open multimodal native mixture-of-experts model. *arXiv preprint arXiv:2410.05993*, 2024b.
- Nikos Manginas, Georgios Paliouras, and Luc De Raedt. NeSyA: Neurosymbolic automata. *arXiv preprint arXiv:2412.07331*, 2024.
- Noushin Mehdipour, Matthias Althoff, Radboud Duintjer Tebbens, and Calin Belta. Formal methods to comply with rules of the road in autonomous driving: State of the art and grand challenges. *Automatica*, 152:110692, 2023.
- OpenGVLab. InternVL 2.0: A suite of multimodal large language models for vision and language tasks. <https://internvl.github.io/blog/2024-07-02-InternVL-2.0/>, 2024.
- Jinhyung Park, Kanchana Ranasinghe, Kumara Kahatapitiya, Wonhyuk Ryu, Donghyun Kim, and Michael S Ryoo. Too many frames, not all useful: Efficient strategies for long-form video QA. *arXiv preprint arXiv:2406.09396*, 2024.
- Aniruddh Puranic, Jyotirmoy Deshmukh, and Stefanos Nikolaidis. Learning from demonstrations using signal temporal logic. In *Conference on Robot Learning (CoRL)*, pages 2228–2242. PMLR, 2021.
- Alec Radford, Jong Wook Kim, Chris Hallacy, Aditya Ramesh, Gabriel Goh, Sandhini Agarwal, Girish Sastry, Amanda Askell, Pamela Mishkin, Jack Clark, et al. Learning transferable visual models from natural language supervision. In *International Conference on Machine Learning (ICML)*, pages 8748–8763. PMLR, 2021.
- Sahil Shah, Harsh Goel, Sai Shankar Narasimhan, Minkyu Choi, S P Sharan, Oguzhan Akcin, and Sandeep Chinchali. A challenge to build neuro-symbolic video agents. In *Proceedings of the International Conference on Neuro-symbolic Systems*, volume 288 of *Proceedings of Machine Learning Research*, pages 676–692. PMLR, 2025a.

- Sahil Shah, S P Sharan, Harsh Goel, Minkyu Choi, Mustafa Munir, Manvik Pasula, Radu Marculescu, and Sandeep Chinchali. NeuS-QA: Grounding long-form video understanding in temporal logic and neuro-symbolic reasoning. *arXiv preprint arXiv:2509.18041*, 2025b.
- S P Sharan, Minkyu Choi, Sahil Shah, Harsh Goel, Mohammad Omama, and Sandeep Chinchali. Neuro-symbolic evaluation of text-to-video models using formal verification. In *Proceedings of the IEEE/CVF Conference on Computer Vision and Pattern Recognition (CVPR)*, pages 8395–8405, 2025.
- Yasser Shoukry, Pierluigi Nuzzo, Ayca Balkan, Indranil Saha, Alberto L Sangiovanni-Vincentelli, Sanjit A Seshia, George J Pappas, and Paulo Tabuada. Linear temporal logic motion planning for teams of underactuated robots using satisfiability modulo convex programming. In *IEEE 56th Annual Conference on Decision and Control (CDC)*, pages 1132–1137. IEEE, 2017.
- Enxin Song, Wenhao Chai, Tiantian Ye, Jae-Ni Hwang, Xi Li, and Guangtao Wang. MovieChat+: Question-aware sparse memory for long video question answering. *arXiv preprint arXiv:2404.17176*, 2024.
- Makarand Tapaswi, Yukun Zhu, Rainer Stiefelhagen, Antonio Torralba, Raquel Urtasun, and Sanja Fidler. MovieQA: Understanding stories in movies through question-answering. In *Proceedings of the IEEE Conference on Computer Vision and Pattern Recognition (CVPR)*, pages 4631–4640, 2016.
- Xiaohan Wang, Yuhui Zhang, Orr Zohar, and Serena Yeung-Levy. VideoAgent: Long-form video understanding with large language model as agent. In *European Conference on Computer Vision (ECCV)*, pages 58–76. Springer, 2024.
- Ziyang Wang, Shoubin Yu, Elias Stengel-Eskin, Jaehong Yoon, Feng Cheng, Gedas Bertasius, and Mohit Bansal. VideoTree: Adaptive tree-based video representation for LLM reasoning on long videos. In *Proceedings of the IEEE/CVF Conference on Computer Vision and Pattern Recognition (CVPR)*, pages 3272–3283, 2025.
- Chao-Yuan Wu and Philipp Krähenbühl. Towards long-form video understanding. In *Proceedings of the IEEE/CVF Conference on Computer Vision and Pattern Recognition (CVPR)*, pages 1884–1894, 2021.
- Haoning Wu, Dongxu Li, Bei Chen, and Junnan Li. LongVideoBench: A benchmark for long-context interleaved video-language understanding. In *Advances in Neural Information Processing Systems (NeurIPS)*, volume 37, pages 28828–28857, 2024.
- Yu Xiong, Qingqiu Huang, Lingfeng Guo, Hang Zhou, Bolei Zhou, and Dahua Lin. A graph-based framework to bridge movies and synopses. In *IEEE/CVF International Conference on Computer Vision (ICCV)*, pages 4591–4600, 2019.
- Yunhao Yang, Jean-Raphaël Gaglione, Sandeep Chinchali, and Ufuk Topcu. Specification-driven video search via foundation models and formal verification. *arXiv preprint arXiv:2309.10171*, 2023.

Jinhui Ye, Zihan Wang, Haotian Sun, Keshigeyan Chandrasegaran, Zane Durante, Cristobal Eyza-guirre, Yonatan Bisk, Juan Carlos Niebles, Ehsan Adeli, Li Fei-Fei, et al. Re-thinking temporal search for long-form video understanding. In *Proceedings of the IEEE/CVF Conference on Computer Vision and Pattern Recognition (CVPR)*, pages 8579–8591, 2025.

Yunan Ye, Zhou Zhao, Yimeng Li, Long Chen, Jun Xiao, and Yueting Zhuang. Video question answering via attribute-augmented attention network learning. In *Proceedings of the 40th International ACM SIGIR Conference on Research and Development in Information Retrieval*, pages 829–832, 2017.

Kaichen Zhang, Bo Li, Peiyuan Zhang, Fan Pu, Joshua Adrian Cahyono, Kaiyang Hu, Shuai Liu, Yuanhan Zhang, Jingkang Yang, Chunyuan Li, et al. LMMS-Eval: Reality check on the evaluation of large multimodal models. *arXiv preprint arXiv:2407.12772*, 2024.

Xin Zheng, Zhen Li, Ivan Ruchkin, Ruzica Piskac, and Miroslav Pajic. NeuroStrata: Harnessing neurosymbolic paradigms for improved design, testability, and verifiability of autonomous CPS. *arXiv preprint arXiv:2502.12267*, 2025.

Junjie Zhou, Yan Shu, Bo Zhao, Boya Wu, Zhengyang Liang, Shitao Xiao, Minghao Qin, Xi Yang, Yongping Xiong, Bo Zhang, Tiejun Huang, and Zheng Liu. Mlvu: Benchmarking multi-task long video understanding. *arXiv preprint arXiv:2406.04264*, 2025.

Yuke Zhu, Oliver Groth, Michael Bernstein, and Li Fei-Fei. Visual7W: Grounded question answering in images. In *Proceedings of the IEEE Conference on Computer Vision and Pattern Recognition (CVPR)*, pages 4995–5004, 2016.

Appendix A.

Proposition 10 (Speedup over Baseline) *The theoretical speedup of LE-NeuS over the baseline NeuS-QA implementation computed as $\frac{\mathcal{L}_{\text{auto}}^{\text{seq}}}{\mathcal{L}_{\text{auto}}^{\text{LE-NeuS}}} \approx \frac{|\mathcal{P}|}{\alpha\rho} \cdot \frac{1}{1 + \frac{T \cdot \mathcal{L}_{\text{CLIP}}}{N_{\text{win}} \cdot \mathcal{L}_{\text{VLM}}}}$.*

Derivation: The speedup follows from comparing the total VLM inference operations required by each method. The baseline processes all $\lceil \frac{T}{\kappa} \rceil$ windows with $|\mathcal{P}|$ sequential passes per window, yielding a total workload proportional to $N_{\text{win}} \cdot |\mathcal{P}|$. Conversely, LE-NeuS restricts the search space to a fraction $\alpha\rho$ of the total windows ($N_{\text{kept}} = \alpha\rho N_{\text{win}}$) and executes exactly one batched proposition detection pass per retained window. Consequently, the primary speedup ratio simplifies to $\frac{|\mathcal{P}|}{\alpha\rho}$. The second term ($\frac{1}{1 + \frac{T \cdot \mathcal{L}_{\text{CLIP}}}{N_{\text{win}} \cdot \mathcal{L}_{\text{VLM}}}}$) accounts for the CLIP scanning overhead, which remains negligible compared to the reduction in VLM calls.